Supporting Information

1. Experimental section

1.1 Materials

Activated carbon (AC), Super P and carbon nanotubes (CNTs) were supplied by Nanjing XFNANO Materials TECH Co., Polyvinylidene difluoride (PVDF) was purchased from Kejin Co., Ltd. V_2O_5, polyvinyl alcohol (PVA) and $Zn(CF_3SO_3)_2$ were provided by Shang Aladdin Biochemical Co., Ltd. $Ni(CH_3COO)_2{\cdot}4H_2O$, $ZnSO_4$, ethyl alcohol (EtOH) and Zn were obtain from Sinopharm Chemical Reagent Co., Ltd. The photosensitive resin materials (Grey Resin v4 and Flexible 80A v1) were supplied by Formlabs Inc.

1.2 Material preparation

$Ni_{0.25}V_2O_5{\cdot}0.88H_2O$ (NiVO) synthesis: Firstly, 4 mmol $Ni(CH_3COO)_2{\cdot}4H_2O$ and 8 mmol V_2O_5 were added into 120 mL distilled water. The mixed solution was gradually heated to 70 ^oC under vigorous stirring. Then, 4 mL EtOH and 6 mL acetone was added into above solution drop by drop. The mixed solution was continuous stirred for 2 hours at 70 ^oC. Afterwards, the stirred solution was transferred into the autoclave for hydrothermal reaction at 200 ^oC for 24 hours. Finally, the obtained products were washed with deionized water and EtOH respectively, and dried in the 70 ^oC oven for the NiVO powder.

Gel electrolyte preparation: 14.5 g $Zn(CF_3SO_3)_2$ was added into 14 mL deionized water and dissolved completely. Then, 2 g PVA was added into the solution and stirred for 2 hours at 70 ^oC for gel electrolyte.

3D printing of stamps: 3D stamps with interdigital patterns were designed with computer aided design (CAD) model and 3D printed by Formlabs Form 3 printer. After printing, as-printed stamps were ultrasonically washed by EtOH and cured for 1 hour by ultraviolet light.

Ink fabrication: AC-based inks composed of 300 mg AC, 40 mg CNTs, 40 mg Super P.NiVO-based inks composed of 300 mg NiVO, 40 mg CNTs, 40 mg Super P. By wet grinding, above materials were mixed. Then, 40 mg PVDF and 1.5 mL NMP were added into AC-based powder to form AC-based inks. 40 mg PVDF and 1.2 mL NMP were added into NiVO-based powder form NiVO based inks. Finally, inks with suitable rheological properties were obtained with the Speed Mixer.

1.3 Fabrication of HZICs

To fabricate HZICs, Ag current collector was firstly stamped onto the PET substrate. Then, AC-based and NiVO-based fingers were stamped onto the one side of Ag current collector layer. After post processes such as soaking and freezing drying, the electrode structures were obtained. On the other side, zinc nanosheet anode was electrodeposited at the current of 15 mA cm^{-2} for 1200 s in 2 M aqueous $ZnSO_4$ solution, using a two-electrode system, where Zn foil and Ag current collector worked as the counter electrode and working electrode, respectively. N/P ratio was ~1:1 (in weight) in a HZIC device in a 2 mm cathode-finger width, and the electrolyte was injected into a 3D printed sealed case.

1.4 Structural characterization and electrochemical measurements

Scanning electron microscopy (SEM) and energy dispersive spectroscopy (EDS) results were collected by Hitachi SU8010 field-emission scanning electron microscope. X-ray diffraction (XRD) patterns were collected by Bruker D8-Advance X-ray diffractometer with Cu Kα ray (λ = 1.540598 Å)

diffraction. X-ray photoelectron spectroscopy (XPS) measurement was conducted by Thermo Scientific K-ALPHA. Galvanostatic charge-discharge (GCD) profiles, cycling stability and rate performance were tested by LAND CT2001A battery test system. Electrochemical impedance spectroscopy (EIS) curves (ranging from 0.01 Hz to 100 kHz) and cyclic voltammetry (CV) curves were tested by CHI 760E electrochemical workstation.

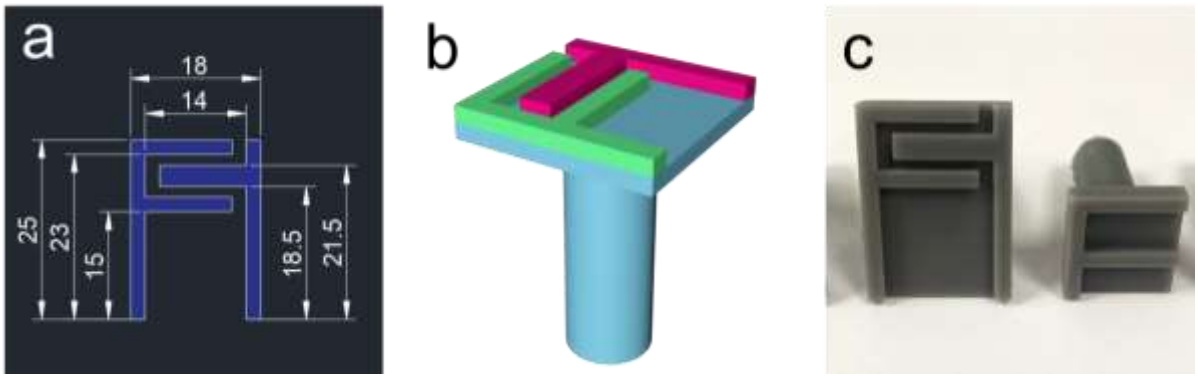

Fig. S1 (a-c) Schematics (a,b) and digital image (c) of 3D printed stamps.

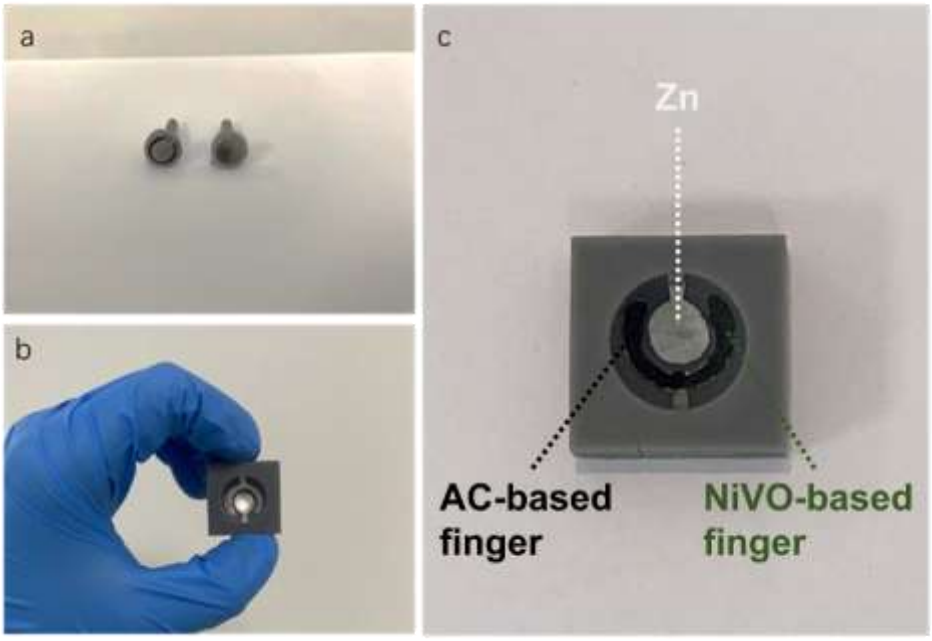

Fig. S2 (a-c) Digital images of 3D semicircular stamps (a), Ag current collector in semicircular plane (b) and HZICs in semicircular plane (c).

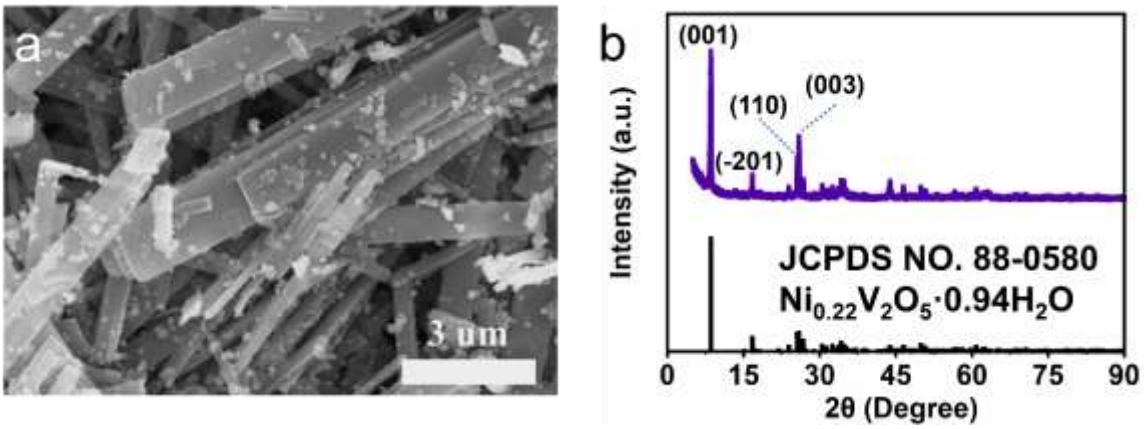

Fig. S3 (a,b) SEM image (a) and XRD pattern (b) of NiVO powder.

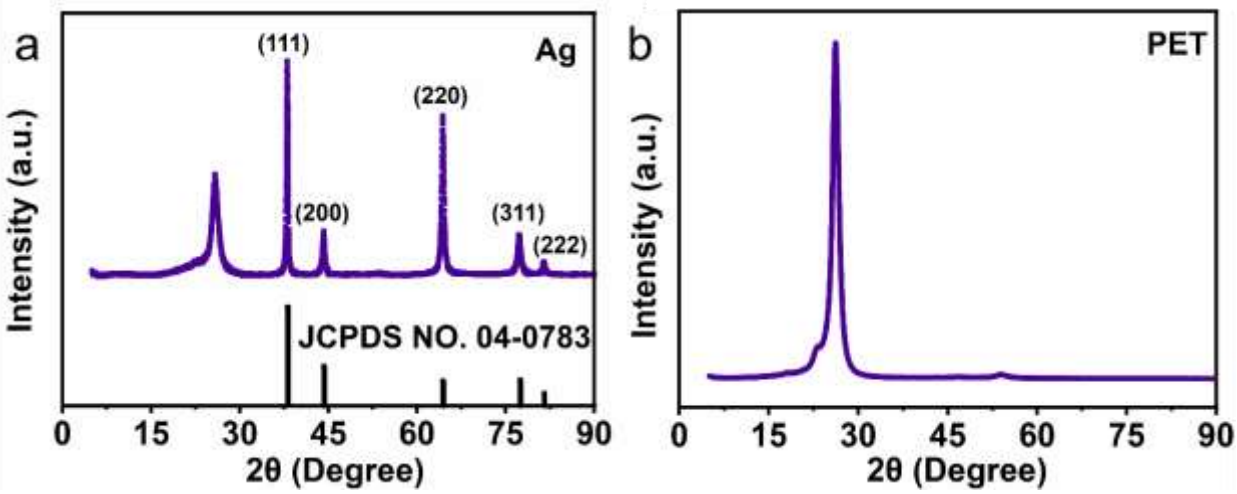

Fig. S4 XRD patterns of (a) Ag current collector and (b) PET.

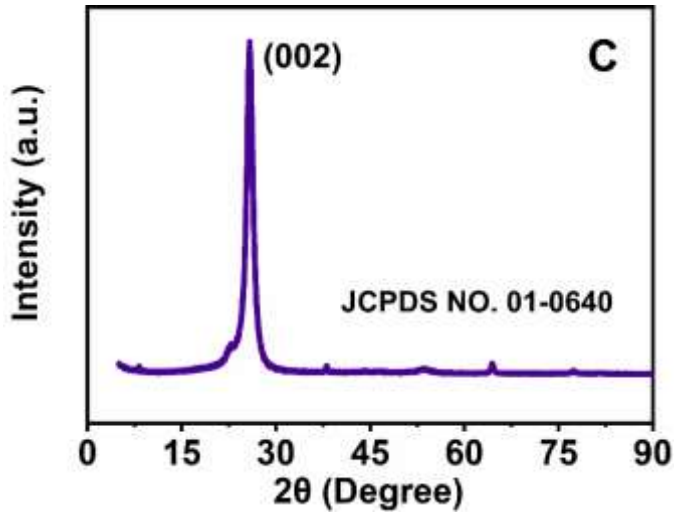

Fig. S5 XRD pattern of AC-based finger.

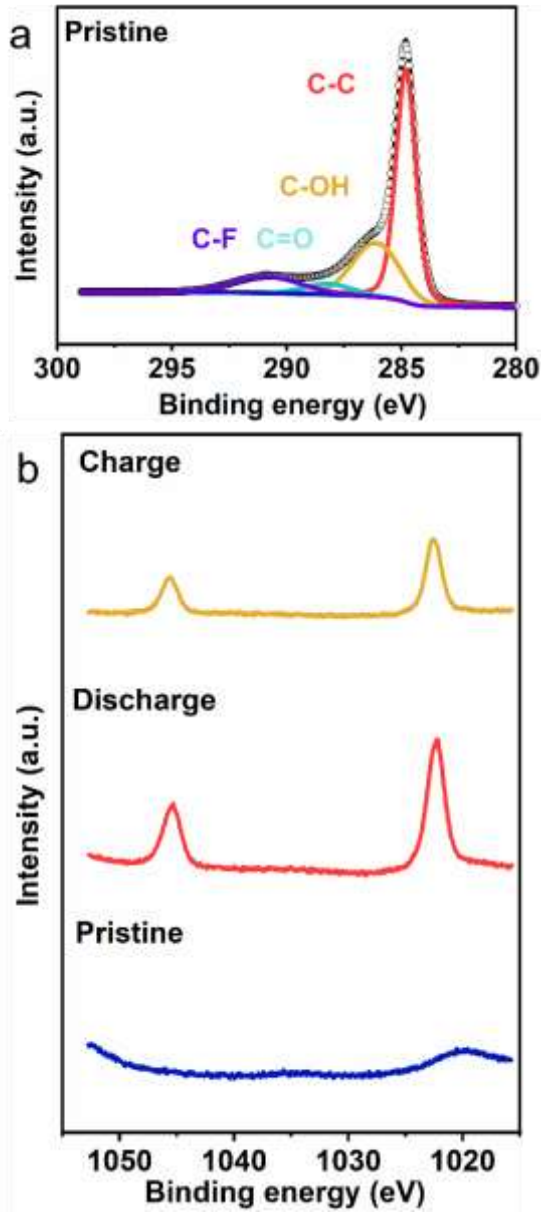

Fig. S6 High-resolution XPS spectra of (a) AC-based finger for C 1s and (b) NiVO-based finger for Zn 2p.

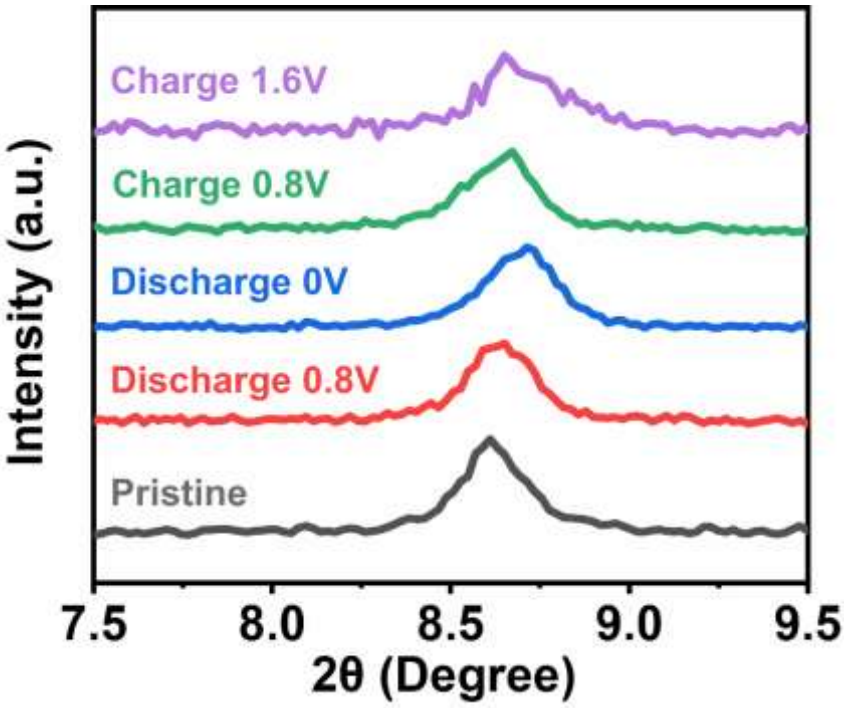

Fig. S7 *Ex situ* XRD patterns of NiVO-based finger of HZICs at different stages.

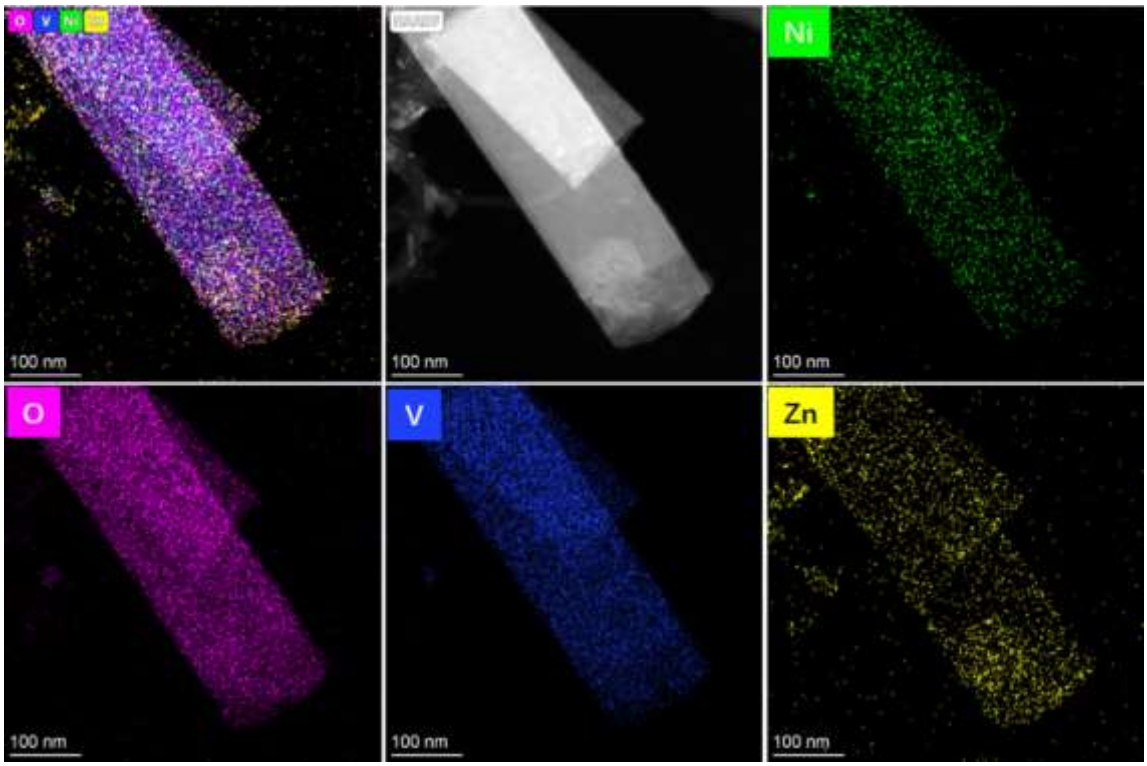

Fig. S8 TEM-EDS element mapping of NiVO at a fully discharged state.

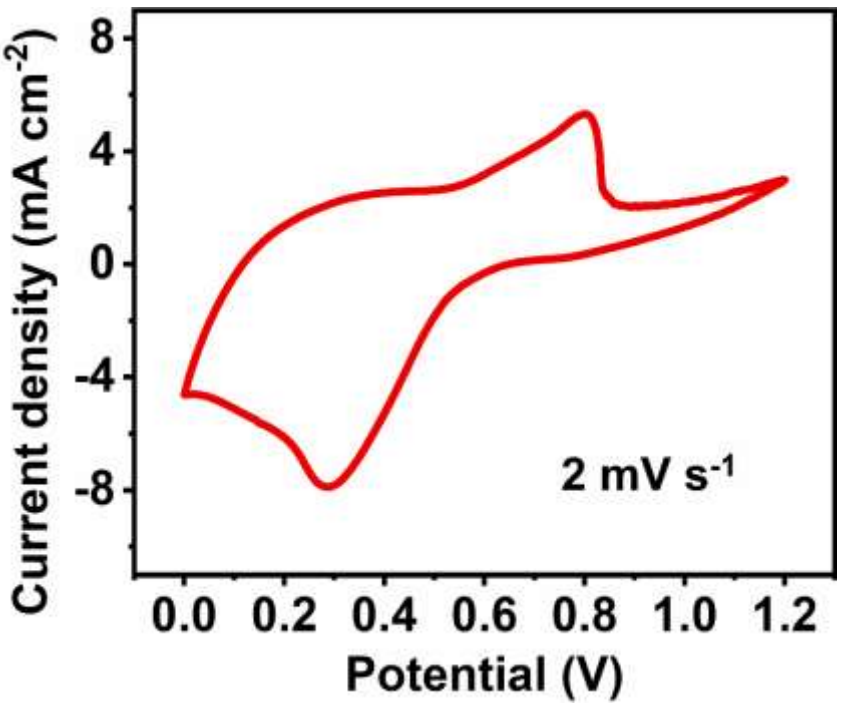

Fig. S9 CV curve of NiVO material tested in three-electrode system using Zn based electrolyte.

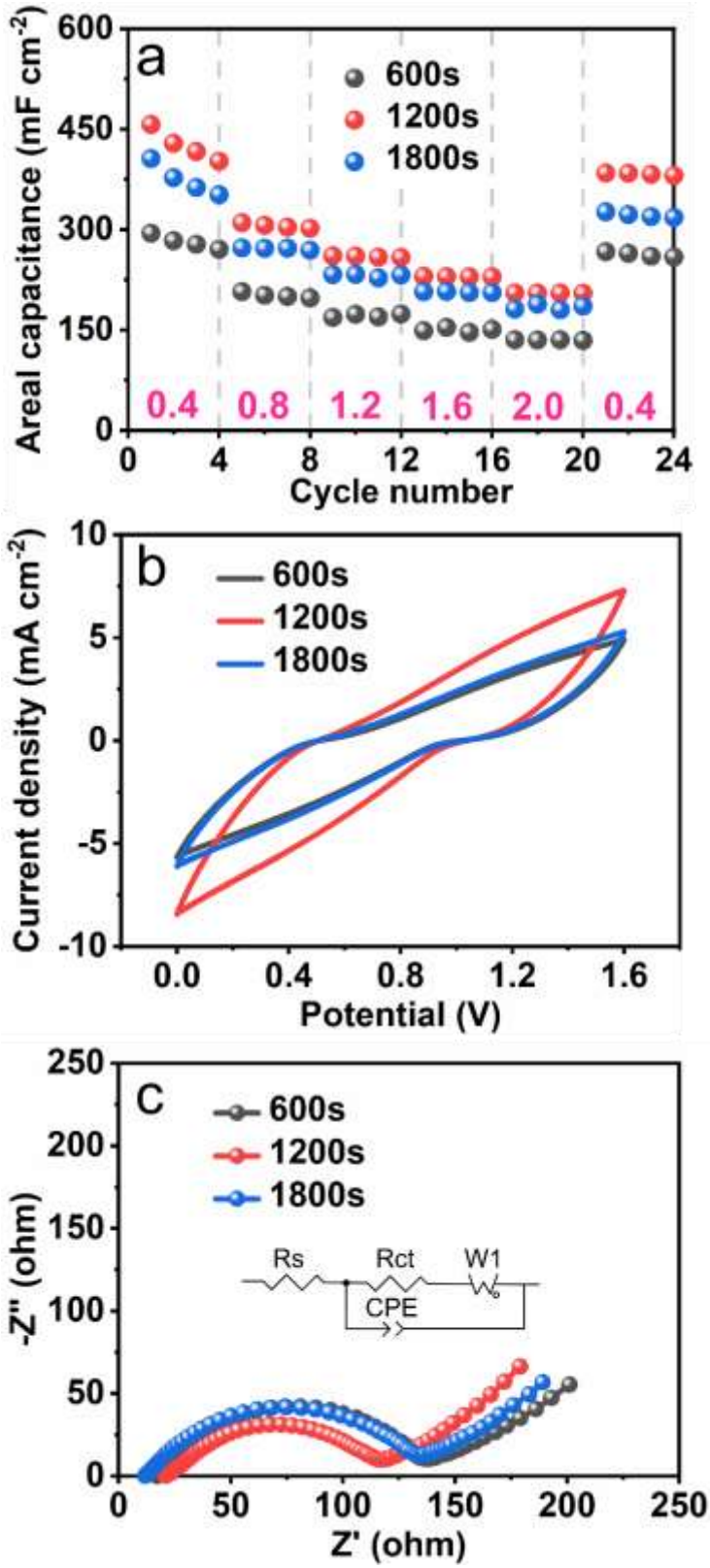

Fig. S10 (a-c) Rate capability (a), CV curves (b) and EIS spectra (c) of HZICs with the different electrodeposition time.

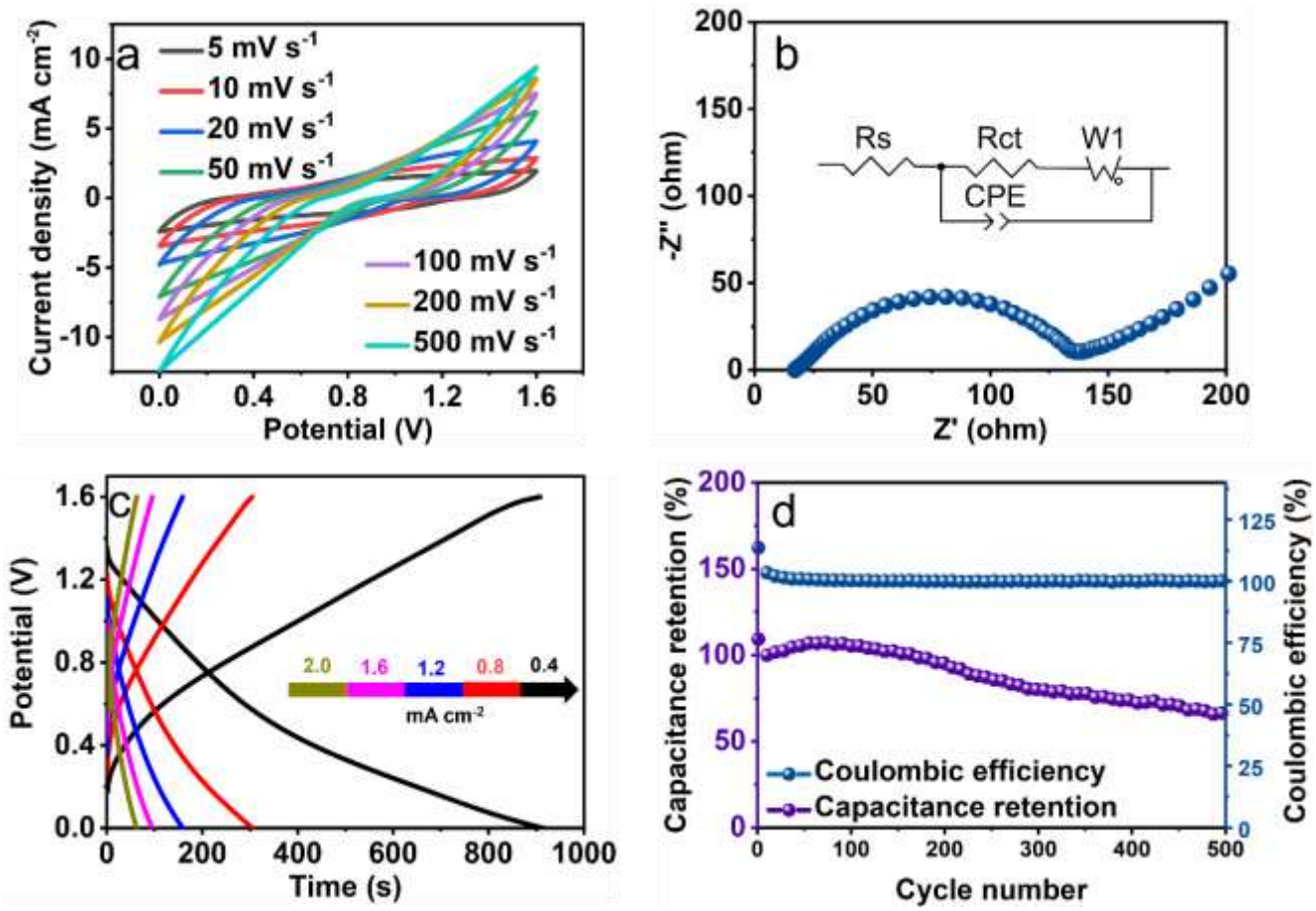

Fig. S11 (a-d) CV curves (a), EIS spectrum (b), GCD profiles (c) and cycling stability (d) of HZICs with the electrodeposition time of 600 s. The value of Rs was 17.9 and the value of Rct was 122.2.

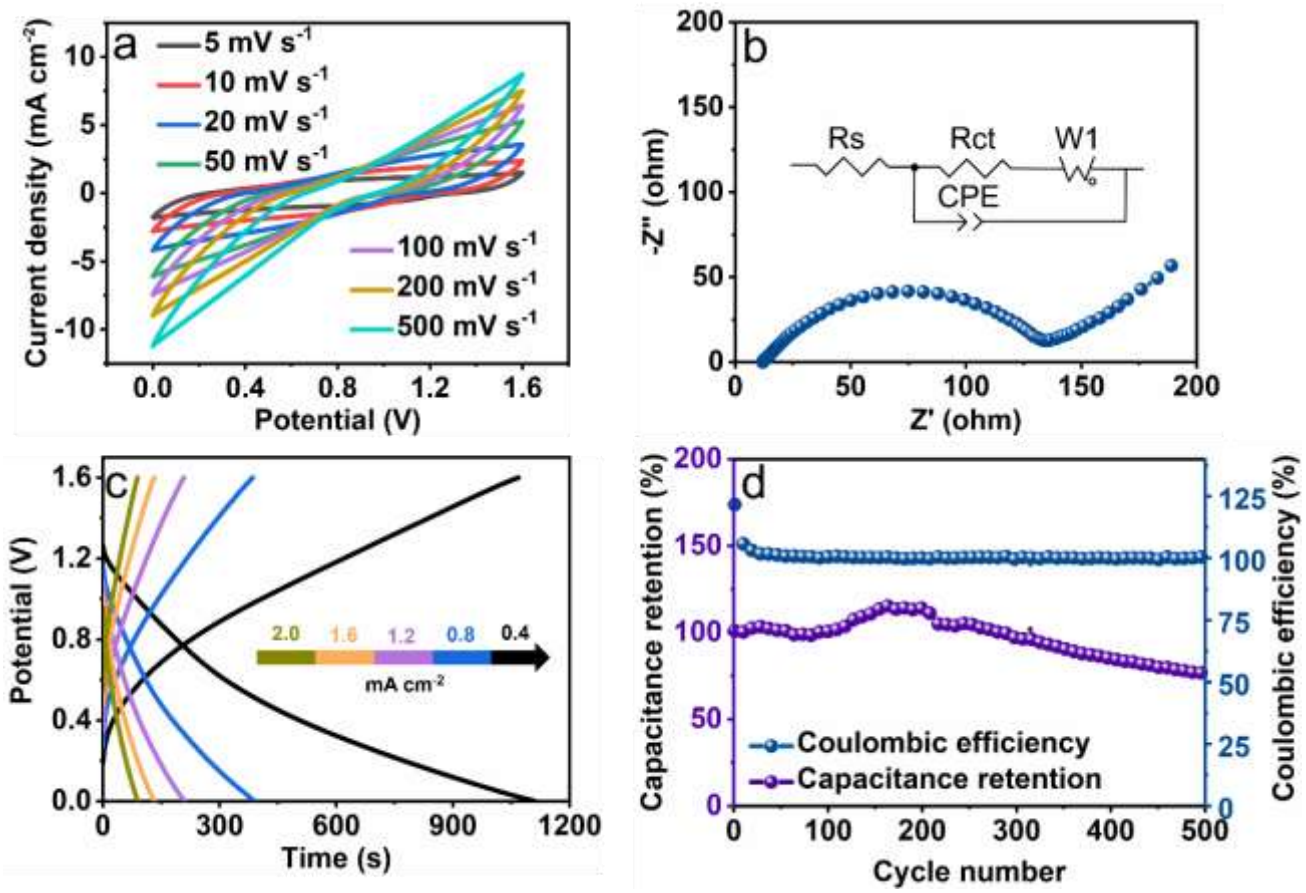

Fig. S12 (a-d) CV curves (a), EIS spectrum (b), GCD profiles (c) and cycling stability (d) of HZICs with the electrodeposition time of 1800 s. The value of Rs was 12.6 and the value of Rct was 121.8.

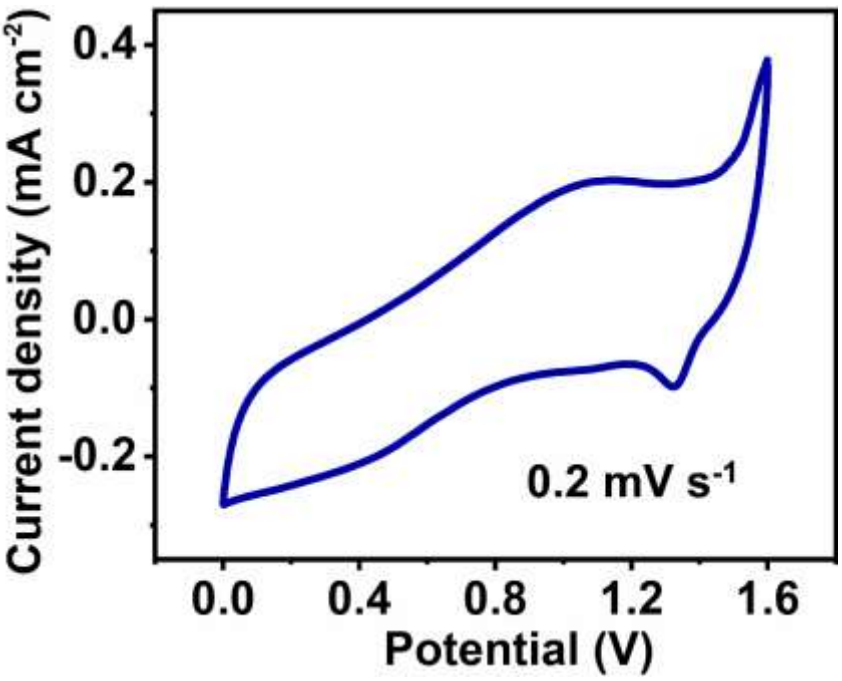

Fig. S13 CV curve of HZICs at a scan rate of 0.2 mV s^{-1}.

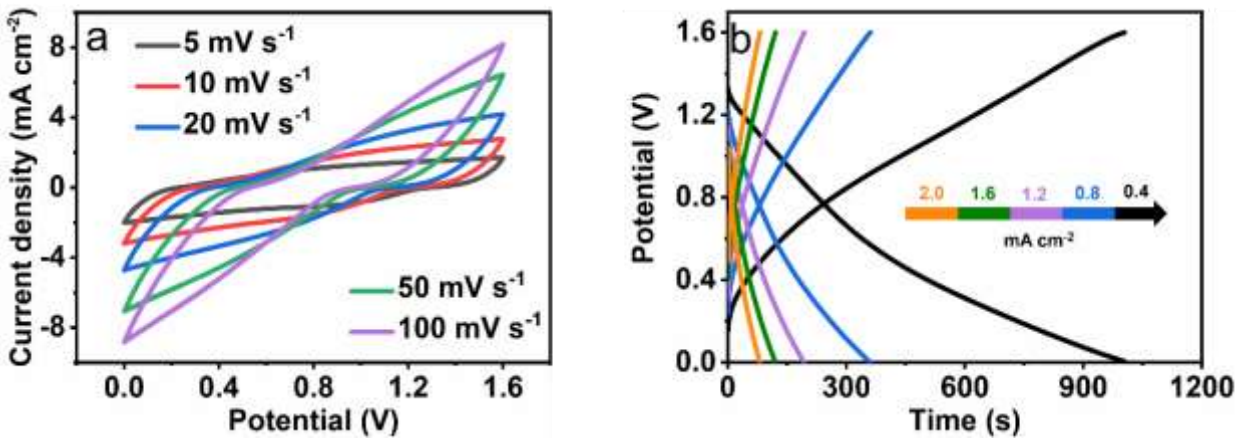

Fig. S14 (a,b) CV curves (a) and GCD profiles (b) of AC-based ZICs.

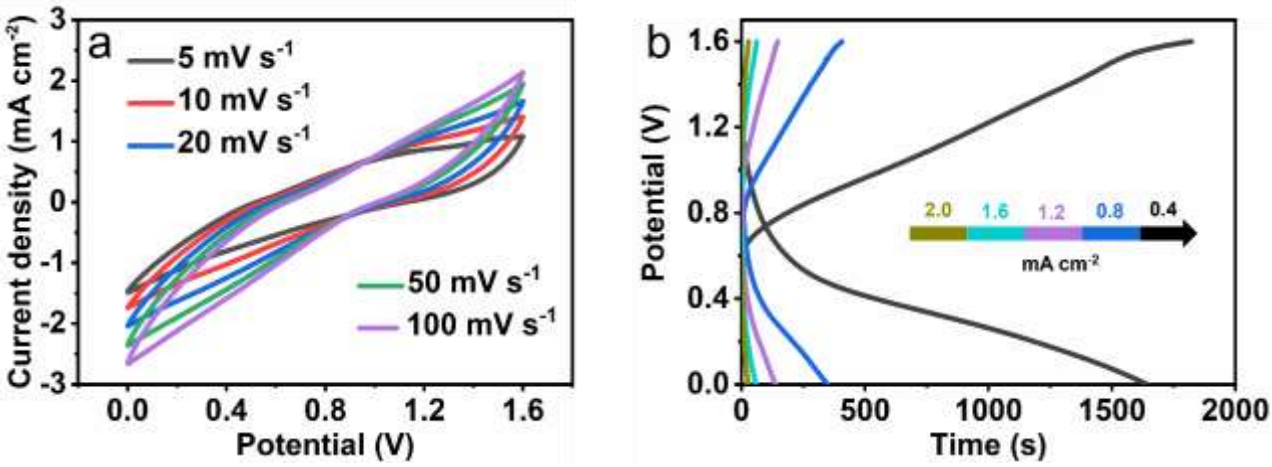

Fig. S15 (a,b) CV curves (a) and GCD profiles (b) of NiVO-based ZIBs.

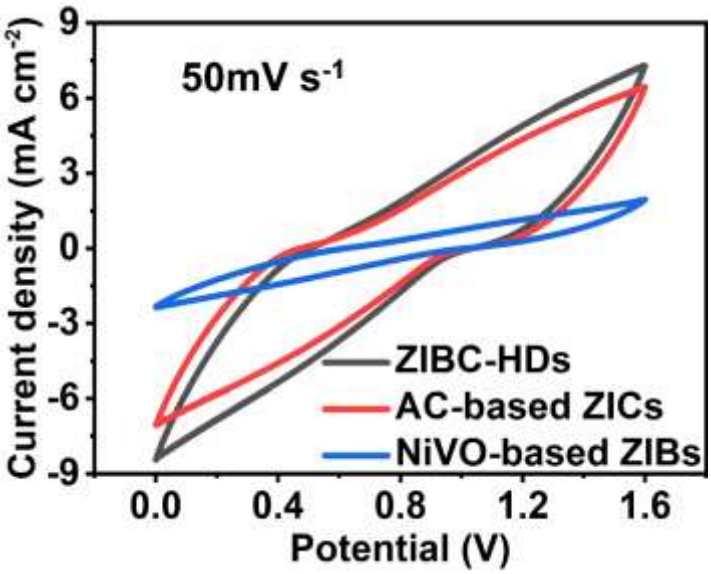

Fig. S16 CV curves of HZICs, bare NiVO-based ZIBs, and bare AC-based ZICs.

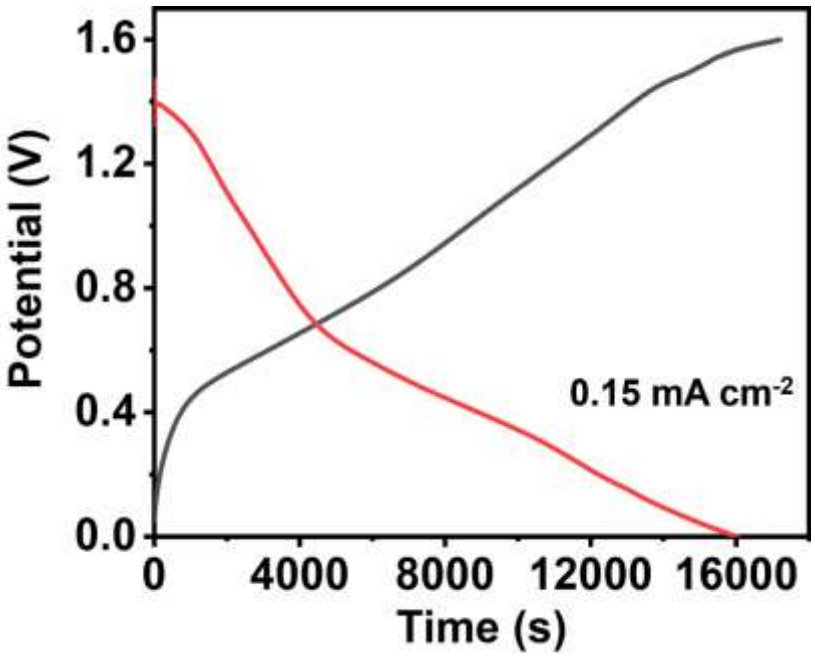

Fig. S17 GCD profiles of HZICs tested at a current density of 0.15 mA cm^{-2}.

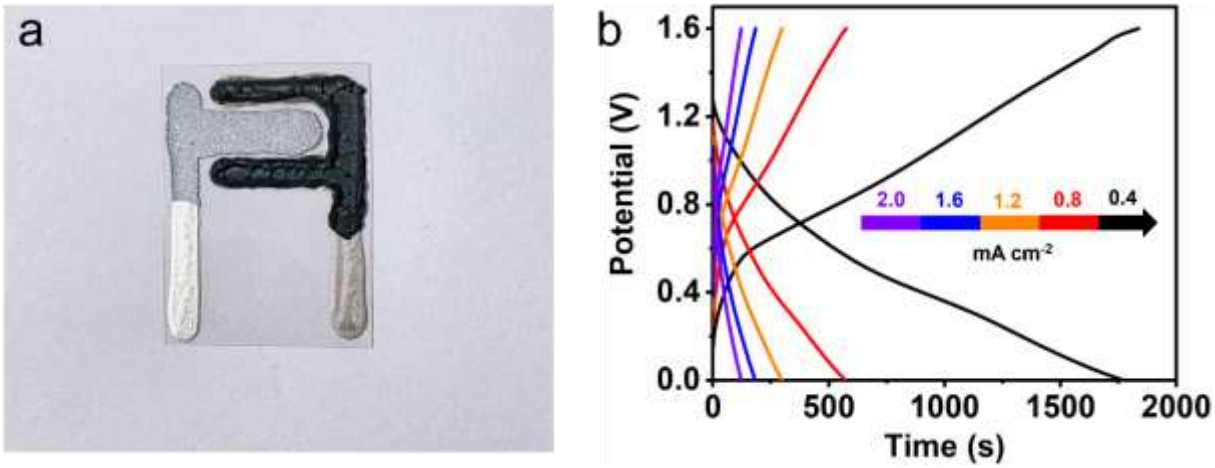

Fig. S18 (a, b) Digital image (a) and GCD profiles (b) of zinc-ion devices with NiVO-AC mixed single cathode and zinc anode.

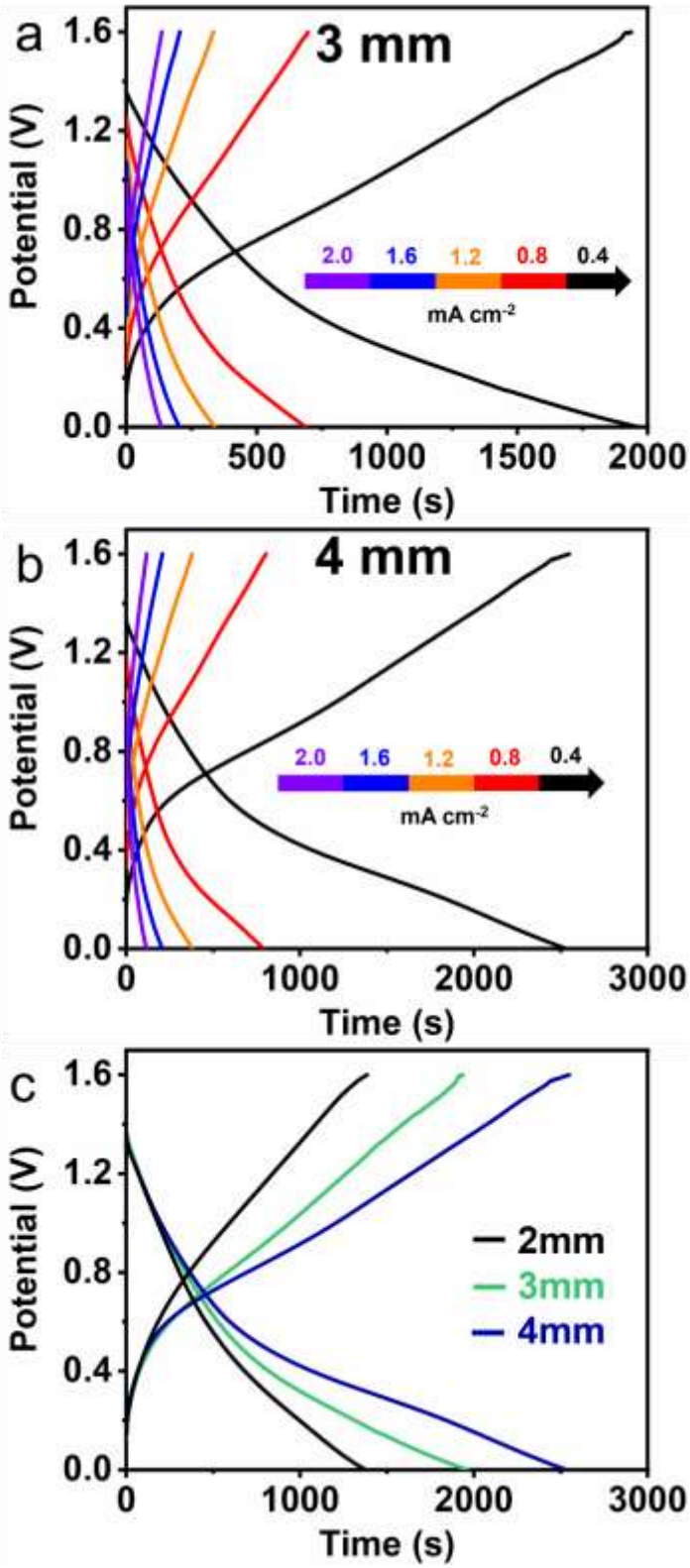

Fig. S19 (a, b) GCD profiles of HZICs with different NiVO-based finger width. (c) GCD profiles of HZICs with different NiVO-based finger width tested at a current density of 0.4 mA cm^{-2}.

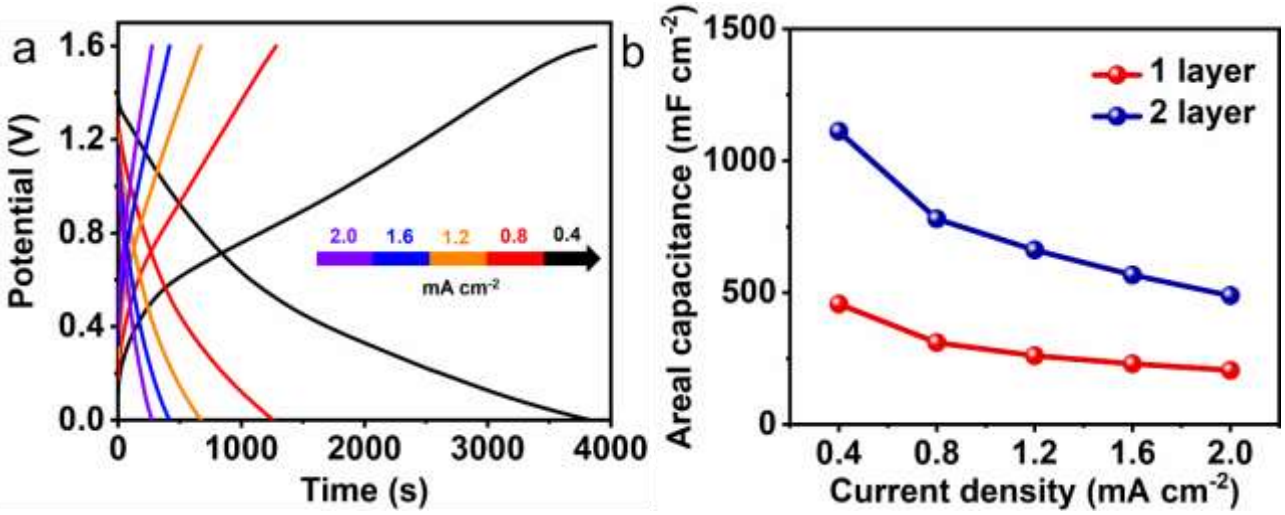

Fig. S20 (a) GCD profiles of HZICs with stamping twice. (b) Areal capacity of stamping once and stamping twice.

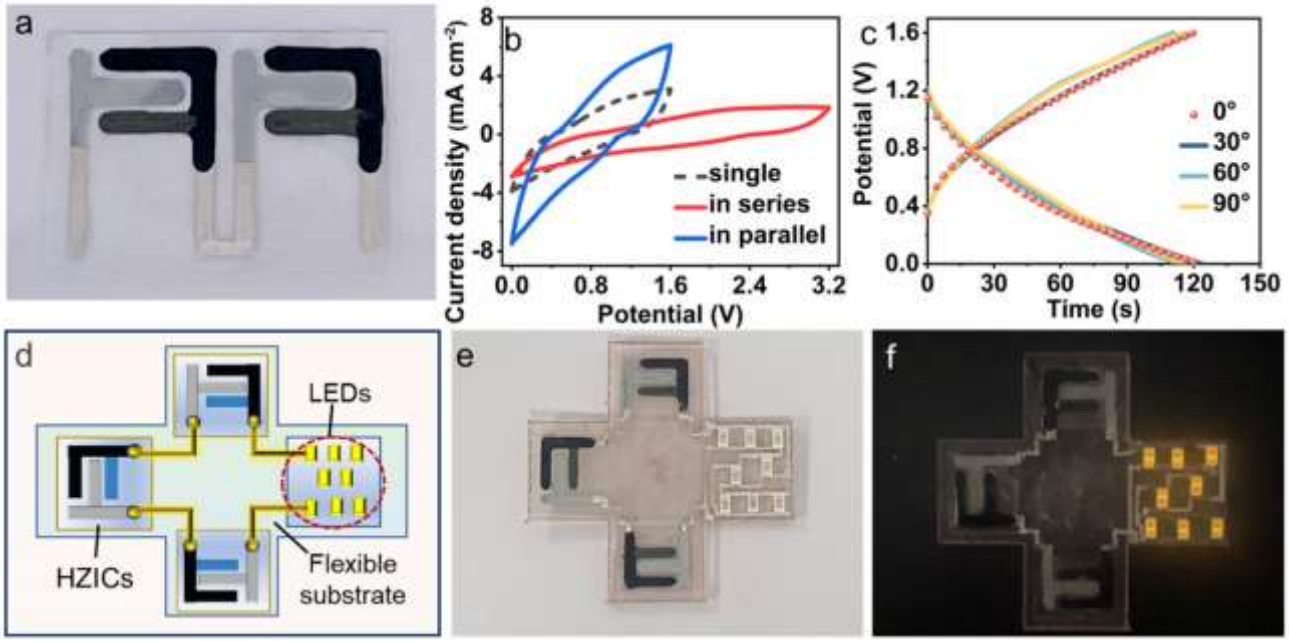

Fig. S21 (a) Photograph of HZICs connected in series. (b) CV curves of the single HZIC, and HZICs in series and parallel way. (c) GCD profiles of HZICs tested at different bending angles. (d, e) Schematic (d) and photograph (e) showing the integration of HZICs and LEDs. (f) Photograph showing that HZICs can easily power the LEDs onto flexible substrates.

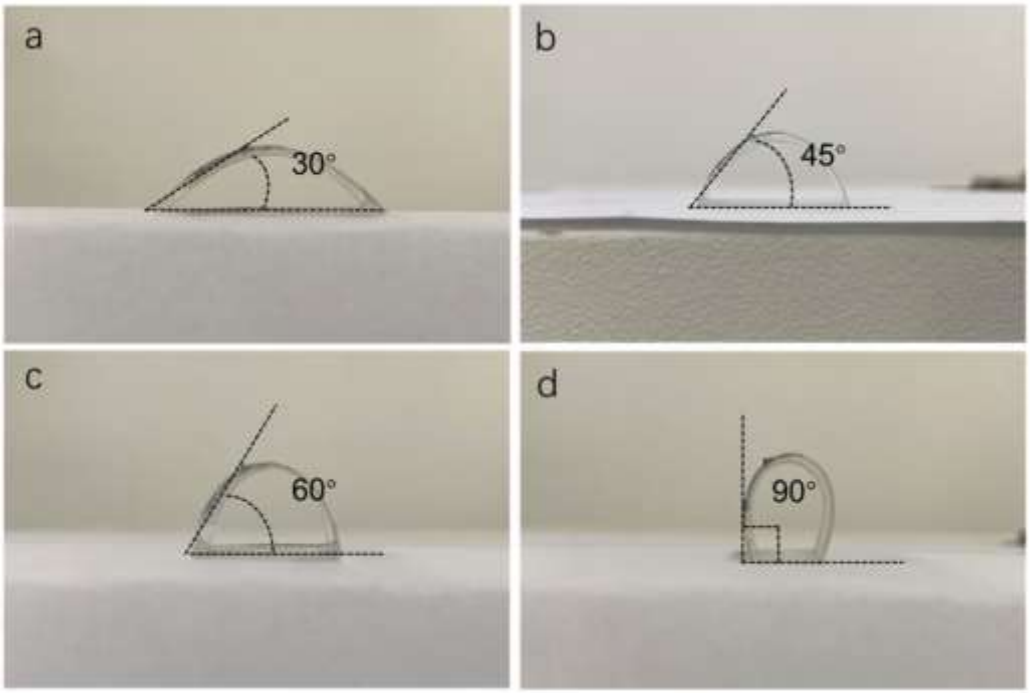

Fig. S22 (a-d) Digital images of HZICs at bending angles.